



# The effects of carbon content on the microstructure and elevated temperature tensile strength of a nickel-base superalloy

Chao-Nan Wei<sup>a,\*</sup>, Hui-Yun Bor<sup>b</sup>, Li Chang<sup>a</sup>

<sup>a</sup> Department of Materials Science and Engineering, National Chiao-Tung University, Hsinchu, 30050, Taiwan, ROC

<sup>b</sup> Metallurgy Section, Materials & Electro-Optics Research Division, Chung-Shan Institute of Science and Technology, Lung Tan, 32599, Taiwan, ROC

## ARTICLE INFO

### Article history:

Received 18 September 2009

Received in revised form 30 January 2010

Accepted 15 March 2010

### Keywords:

Carbon

Grain refinement

Nickel-base superalloy

Hot isostatic pressing

Microstructure

Tensile test

## ABSTRACT

This study investigates how carbon content affects the microstructure and elevated temperature tensile strength of fine-grain CM-681LC superalloy. Experimental results indicate that increasing the carbon content from 0.11 to 0.15 wt% increases the total area fraction of carbides considerably. However, the two alloys exhibit similar carbide shapes and sizes, probably because the short solidification time in the fine-grain process limits the growth of carbides. Besides, carbon addition significantly reduces the area fraction of  $\gamma$ - $\gamma'$  eutectic phases from 8.6 to 5.3% because the eutectic phase forming elements are consumed by (Ta, Hf)C carbides and the carbides occupy the position of  $\gamma$ - $\gamma'$  eutectic phases during the solidification. Further, the carbon addition improves the mechanical strength by about 6% and the elongation by about 50% in tensile tests at 760 °C and yields favorable tensile performance at elevated temperature.

© 2010 Elsevier B.V. All rights reserved.

## 1. Introduction

The CM-681LC superalloy, a nickel-base superalloy developed by Cannon-Muskegon (CM) Corporation in the United States of America, exhibits outstanding mechanical properties under high temperature and high stress conditions due to its special alloy design. This superalloy exhibits increased grain boundary strength and ductility when its microstructures are stable. Its enhanced grain boundary strength and ductility allow both directionally solidified columnar grain casting and polycrystal casting [1]. The CM-681LC superalloy has a nominal 0.11 wt% carbon content, which is added to form MC and  $M_{23}C_6$  carbides providing the strengthening effect.

The fine-grain process (FGP) developed by Howmet Corporation uses a controlled low pouring temperature to increase the strength, elongation, and fatigue durability of conventional castings [2]. Fine-grain castings have advantages such as refined carbides and precipitates, enhanced strength, elongation, and improved mechanical properties [3]. Thus, fine-grain processes are beneficial for the strength and fatigue life of castings working at moderate temperatures (427–760 °C).

Carbide plays a complex role in nickel-base superalloys, and its effects on mechanical properties are not clearly understood yet. The literature [4,5] points out that carbon can be a grain boundary (GB)

strengthening element in nickel-base superalloys. The carbon content affects the amount, size, and shape of carbides. If the carbon content is too low, it has a negative effect on mechanical properties due to the formation of the filmy carbides at GBs. On the other hand, if the carbon content is too high, there is also a negative effect on mechanical properties due to the precipitation of script-like and elongated carbides, which allow crack initiation and propagation along carbide/matrix interfaces. Therefore, adding the proper proportion of carbon with the carbide precipitation in the appropriate amount, size, and shape is likely to improve the mechanical properties of nickel-base superalloys [6–10]. Furthermore, the carbon content has a significant effect on the microstructure and mechanical property of conventional polycrystal and single crystal superalloys. But, the effect of carbon addition on the microstructure and mechanical property of fine-grain superalloys is not yet clearly studied.

Though CM-681LC superalloy with 0.11 wt% carbon content can be used in polycrystal and columnar grain casting processes, the optimum carbon content for better mechanical properties of the fine-grain process is not known. However, it is known that the GBs in fine-grain castings are more than in traditional castings. Therefore, the GB strength of fine-grain CM-681LC superalloy may improve by adding carbon content properly to precipitate more carbides at GBs. This study investigates the microstructure and elevated temperature tensile strength of fine-grain samples having 0.11 and 0.15 wt% carbon, and compares them in terms of the carbides,  $\gamma$ - $\gamma'$  eutectic phases, tensile strength and more.

\* Corresponding author. Tel.: +886 3 4712201x357254; fax: +886 3 4111334.  
E-mail address: [chaonien@ms41.hinet.net](mailto:chaonien@ms41.hinet.net) (C.-N. Wei).

**Table 1**  
Chemical compositions of 11C and 15C (unit in wt%).

Test bar no.	Cr	Co	Mo	W	Re	Ta	Al	Ti	Hf	C	B	Zr	Ni
11C	5.5	9.3	0.51	8.4	2.9	6.1	5.71	0.16	1.49	0.11	0.19	0.12	Bal.
15C	5.3	9.3	0.50	8.4	2.8	5.8	5.52	0.12	1.45	0.15	0.19	0.12	Bal.

## 2. Experimental method

The experiments in this study used a CM-681LC nickel-base superalloy ingot as the starting material. Equiaxed fine-grain samples with 0.11 and 0.15 wt% carbon content were cast using the fine-grain process, which has a low pouring temperature. The temperature gradient in the fine-grain process was reduced to limit the growth of fine grains. The pouring and mold temperatures were 1380 and 1100 °C, respectively.

Sample chemical compositions were analyzed using spark emission spectroscopy and carbon-sulphur analyzer. The melting points were measured using differential scanning calorimetry (DSC). To avoid the negative effect of the fine-grain process on mechanical properties due to micropores caused by rapid solidification shrinkage, all samples were treated with hot isostatic pressing (HIP) to reduce micropore density. HIP was performed at 1185 °C under an Ar gas pressure of 172.25 MPa for 5 h. Samples were then subjected to solid solution treatment in a vacuum at 1185 °C for 4 h, followed by cooling in an Ar atmosphere to room temperature. An aging treatment was then performed at 1038 °C for 2 h in a vacuum, before cooling to room temperature in an atmosphere of gaseous Ar. The test specimens were secondarily aged at 871 °C for 20 h in a vacuum and then cooled to room temperature in a furnace. The grain sizes were observed with secondary electron imaging (SEI) using scanning electron microscopy (SEM), and the intercept method was applied to determine grain sizes. The microstructures were characterized by SEM and transmission electron microscopy (TEM). SEM specimens were prepared using standard mechanical polishing procedures and etched in 30 ml lactic acid + 10 ml HNO<sub>3</sub> + 5 ml HCl solution. Twin jet electrolytic etching was employed in 90% CH<sub>3</sub>COOH + 10% HClO<sub>4</sub> solution to prepare TEM specimens. Microanalysis of the specimens was performed with X-ray energy dispersive spectroscopy (EDS) in SEM. In addition, the average length, aspect ratio (the ratio of long axis and short axis), area fraction of carbides and area fraction of  $\gamma$ - $\gamma'$  eutectic phase were analyzed using an image analyzer. One hundred fields from the samples were taken by a 200 times optical microscope to measure the mean value. The tensile tests were performed using an Instron 1125 universal test machine at 760 °C. The gauge size of test bars was 6.3 mm in diameter and 26 mm in length. The fracture morphology was observed using SEM.

## 3. Results

The main compositions of fine-grain test samples with different carbon content were identified by spark emission spectroscopy, and their carbon content was determined using a carbon-sulphur analyzer. Table 1 shows the results. The carbon weight percentages of two alloys, indicated as 11C and 15C, are 0.11 and 0.15%, respectively. DSC analysis shows no significant difference in the melting points of 11C and 15C, which were 1347 and 1351 °C, respectively.

The grain sizes obtained by traditional investment casting process using a pouring temperature of about 1480 °C are 3–5 mm, and their morphology tends to be columnar. Fig. 1 shows the grain sizes of 11C and 15C after HIP and heat treatments. The grain sizes of both 11C and 15C obtained by the fine-grain process in this study are 80  $\mu$ m (Fig. 1(a) and (b)), and the structures of both are

equiaxed, unlike the grain sizes and shapes resulting from the traditional casting process. These results suggest that the carbon content of the samples has a negligible effect on grain size and shape. On the other hand, they indicate that reducing the temperature gradient by lowering the pouring temperature and controlling the mold temperature shortens the solidification time, limiting grain growth.

Fig. 2(a) and (b) show the microstructure of 11C and 15C, respectively, after HIP and heat treatments. The microstructure consists mainly of the matrix  $\gamma$ , reinforced phase  $\gamma'$ , eutectic structure  $\gamma$ - $\gamma'$ , and carbides.

Fig. 3(a) presents the carbide morphology in 11C. The carbides with script-like and blocky morphology within the grain interior are rich in Ta and Hf (Fig. 3(b) and (c)). On the basis of the US patent for CM-681LC superalloy [1], these carbides can be confirmed as MC carbides. Fig. 4(a) shows that particle-like carbides precipitated at GBs in 11C, and EDS analysis demonstrates that they are Cr-rich (Fig. 4(b)), indicating that they are M<sub>23</sub>C<sub>6</sub> carbides. This identification was confirmed by TEM. Fig. 5 presents bright-field and dark-field images of an M<sub>23</sub>C<sub>6</sub> carbide and its selected-area diffraction pattern.

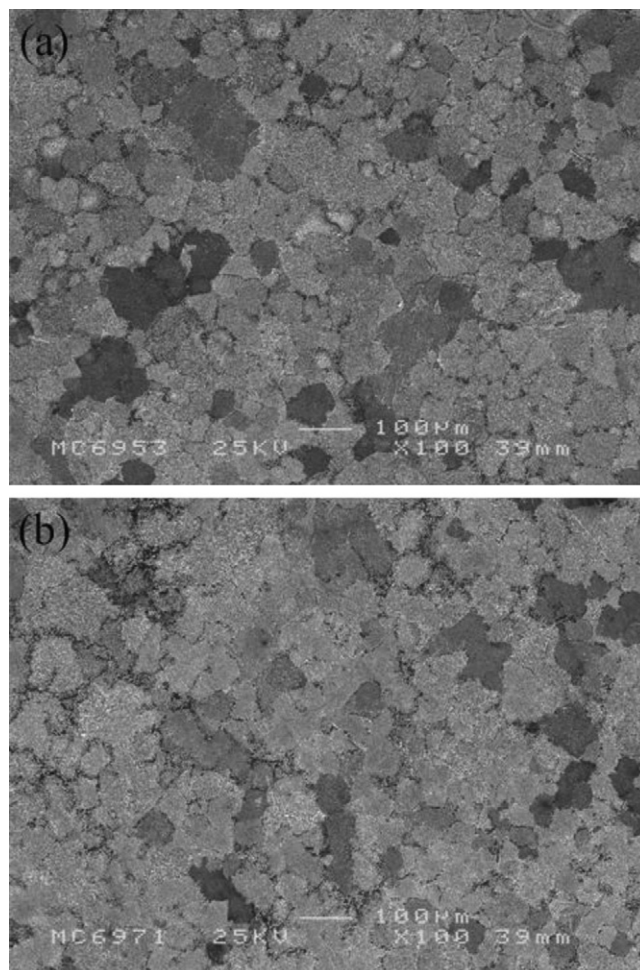


**Fig. 1.** SEM images showing the grain sizes of (a) 11C and (b) 15C after HIP and heat treatment.

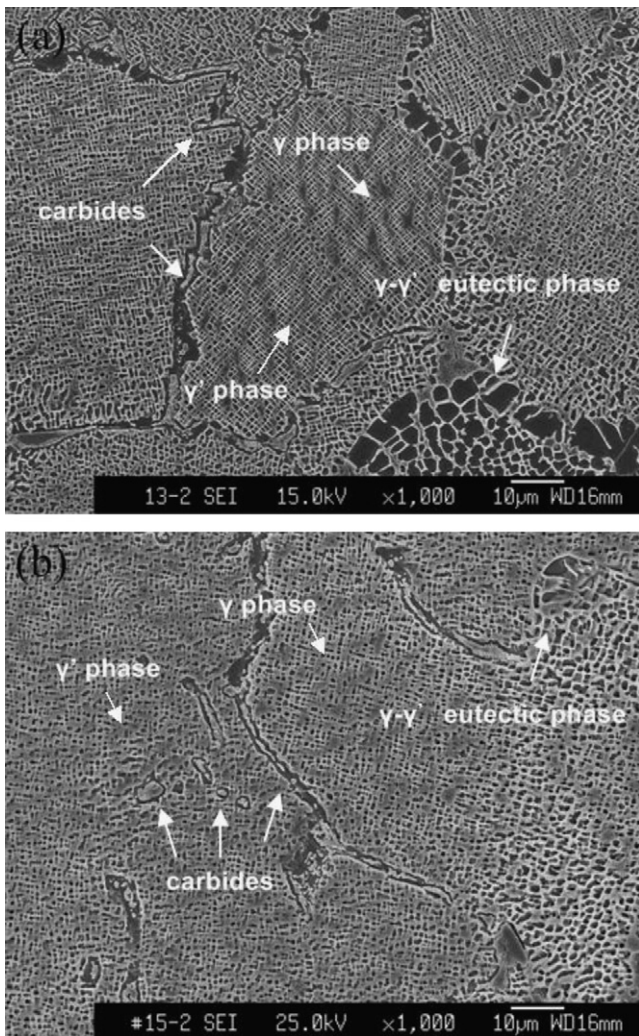


Fig. 2. SEM images showing the microstructure of (a) 11C and (b) 15C after HIP and heat treatment.

Fig. 6(a) shows the carbide morphology in 15C. The EDS analysis shown in Fig. 6(b) shows that the script-like carbide within the grain interior is rich in Ta and Hf, and is MC ((Ta, Hf)C) carbide. The blocky carbide within the grain interior is enriched with Ta and Hf (Fig. 6(c)), and is also MC ((Ta, Hf)C) carbide. The discontinuous particle-like carbide at GBs shown in Fig. 7(a) is Cr-rich (Fig. 7(b)), and is the  $M_{23}C_6$  ( $Cr_{23}C_6$ ) carbide. The same types of carbide occur in 11C and 15C, but their amounts appear to be significantly different. Table 2 presents statistical results for the area fraction, average length, and aspect ratio of carbides in 11C and 15C. It shows that the carbon content increases from 0.11 to 0.15 wt%, and the total area fraction of carbides increases greatly, from 0.91 to 1.57%. Additionally, the average carbide length increases from 12.84 to 13.82  $\mu\text{m}$ , while the aspect ratio increases from 1.85 to 1.96. These experimental results reveal that carbon addition in the fine-grain process can increase the amount of carbide, but no significant differences appear in the size and shape of the carbides.

**Table 2**  
Statistical results for carbide characteristics of 11C and 15C.

Area fraction (%)		Average length ( $\mu\text{m}$ )		Aspect ratio	
11C	15C	11C	15C	11C	15C
0.91	1.57	12.84	13.82	1.85	1.91

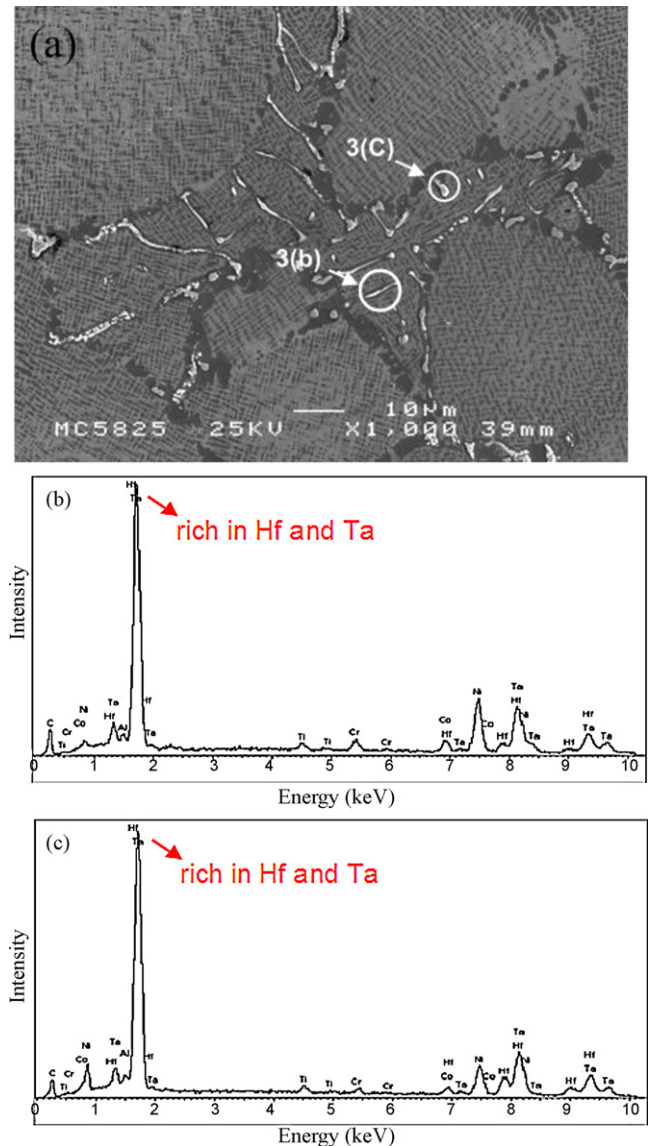


Fig. 3. (a) SEM images showing the carbide morphology in 11C with EDS spectra in (b) and (c) from the carbides arrowed in (a).

Fig. 8(a) and (b) show the  $\gamma$ - $\gamma'$  eutectic phase morphology in 11C and 15C, respectively. The  $\gamma$ - $\gamma'$  eutectic phase usually forms near GBs at the end of the solidification process. The results shown in Fig. 8(c) indicate that the area fractions of this phase in 11C and 15C are 8.6 and 5.3%, respectively. This suggests that carbon addition significantly reduces the area fraction of the  $\gamma$ - $\gamma'$  eutectic phase.

The tensile properties of 11C and 15C tested at 760  $^{\circ}\text{C}$  are listed in Table 3; they show an improvement in tensile properties associated with carbon addition. The ultimate tensile strength and yield strength of 15C are about 6% greater than those of 11C. Furthermore, the elongation is drastically improved from 4.3 to 6.6%. These results show that an increase in carbon content from 0.11 to 0.15 wt% in fine-grain CM-681LC superalloy can improve its tensile performance at 760  $^{\circ}\text{C}$ .

**Table 3**  
Tensile test results of 11C and 15C at 760  $^{\circ}\text{C}$ .

U.T.S. (MPa)		Y.S. (MPa)		Elongation (%)	
11C	15C	11C	15C	11C	15C
1003	1065	945	997	4.3	6.6

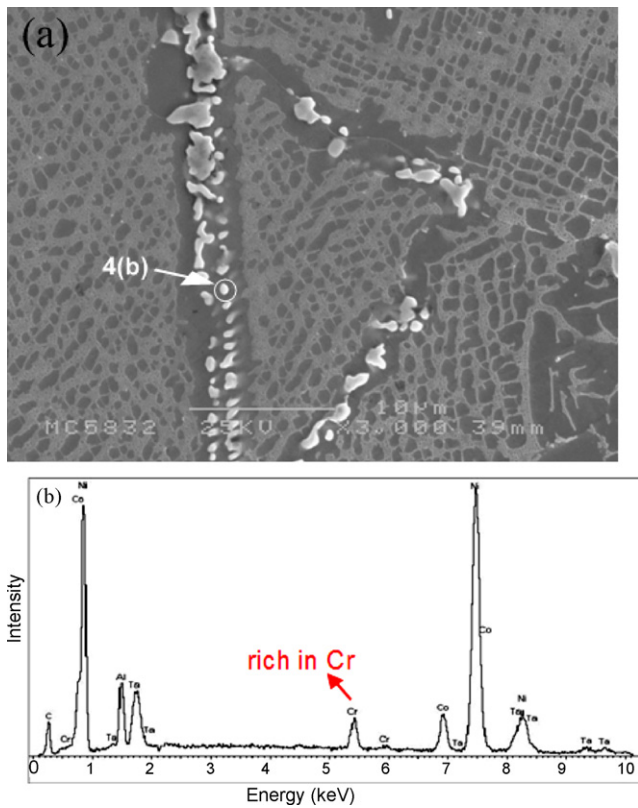


Fig. 4. (a) SEM images showing the carbides at GBs in 11C with EDS spectra in (b) from the carbides arrowed in (a).

Fractographic observations were made using SEM to study the effect of carbon on the tensile fracture morphology of 11C and 15C. The fracture surface of 11C presents that cracks are observed at GBs (Fig. 9(a)), and it is a typical intergranular fracture mode. After carbon was added, the cracks in 15C were distributed mainly at both the GBs and carbide/matrix interfaces (Fig. 9(b)). The fracture surface of 15C appears to be mixed, involving intergranular and transgranular cracks.

#### 4. Discussion

Carbon addition significantly affects the microstructure and elevated temperature tensile strength of fine-grain CM-681LC superalloy. This section discusses the effects of carbon addition on the grain size, carbides,  $\gamma$ - $\gamma'$  eutectic phase, and tensile properties.

##### 4.1. Grain size

The DSC analysis results show no significant difference in the melting points of 11C and 15C. In addition, the grain sizes of 11C and 15C are almost the same, about 80  $\mu\text{m}$ . The temperature gradient between melting point and pouring temperature in the fine-grain process is the main factor affecting grain size. As both alloys share the same temperature gradient, it is reasonable that carbon addition produces no obvious change in grain size.

##### 4.2. Carbides

Carbon plays the role of a GB strengthening element in Ni-base superalloys. Carbon and carbide-forming alloying elements can form carbides within grains and at GBs, and the carbides effectively obstruct the movement of dislocations and inhibit the GB

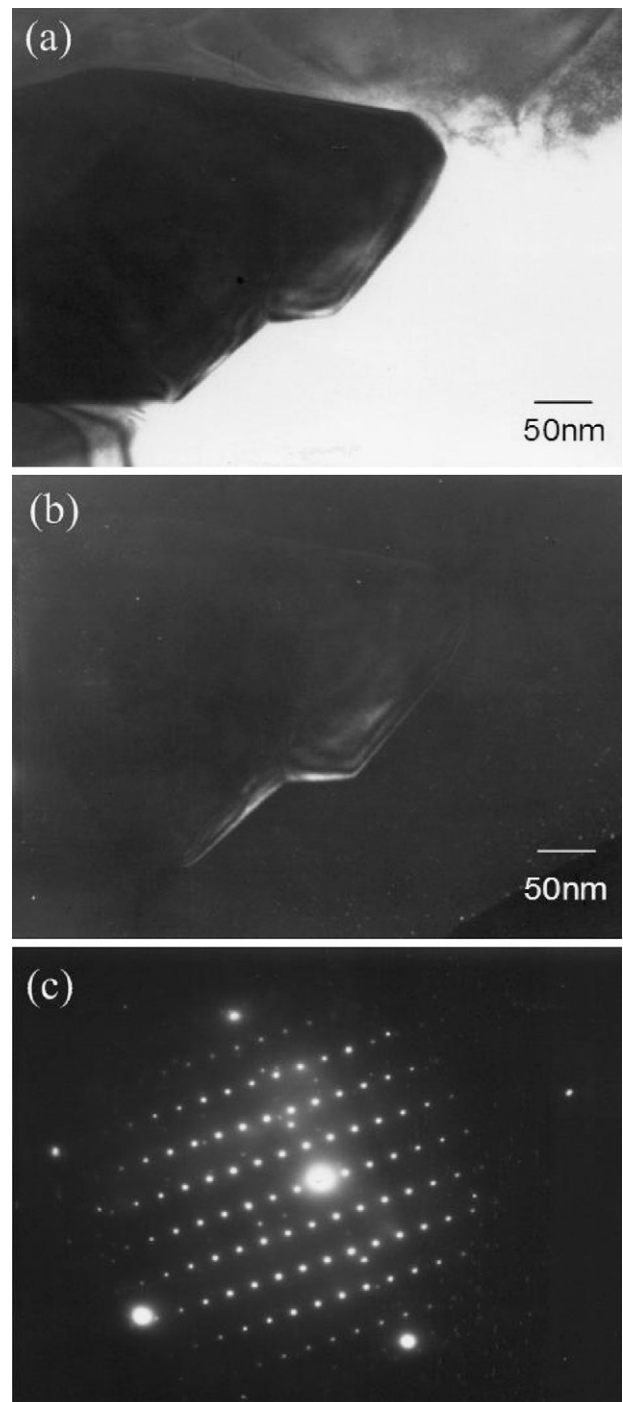
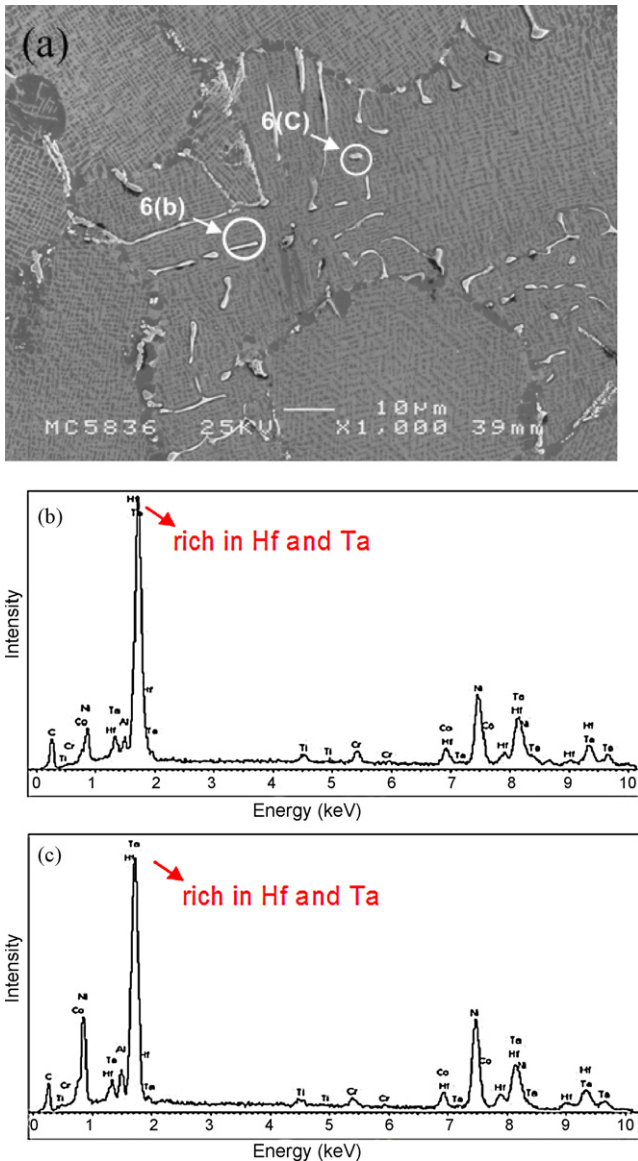


Fig. 5. (a) Bright-field image of a  $\text{Cr}_{23}\text{C}_6$  ( $\text{M}_{23}\text{C}_6$ ) carbide, (b) dark-field image of the carbide, and (c) selected-area diffraction pattern corresponding (a).

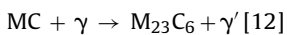
sliding. The strengthening effect of carbides effectively improves the mechanical properties of superalloys [4].

The literature [1,11] indicates that the principal carbides of CM-681LC superalloy are MC carbides precipitated during solidification. The MC carbide in superalloy has a tendency to decompose into  $\text{M}_{23}\text{C}_6$  or  $\text{M}_6\text{C}$  with heat treatment or thermal exposure [10,12–14]. Generally, the  $\text{M}_{23}\text{C}_6$  carbides are rich in Cr and the  $\text{M}_6\text{C}$  carbides are rich in Mo or W [10,12,13]. The EDS and TEM analysis results indicate that MC carbides in CM-681LC superalloy were transformed to discontinuous particle-like  $\text{M}_{23}\text{C}_6$  carbides at



**Fig. 6.** (a) SEM images showing the carbide morphology in 15C with EDS spectra in (b) and (c) from the carbides arrowed in (a).

the GBs after HIP and heat treatment.



Hence, the main carbides in 11C are script-like or blocky (Ta, Hf)-rich MC phase and particle-like Cr-rich  $M_{23}C_6$  phase.

The added carbon easily reacts with carbide-forming elements such as Ta and Hf to form extra MC carbides during solidification. According to the EDS analysis shown in Fig. 6(b) and (c), the carbides with script-like and blocky morphology within the grain interior in 15C are MC carbides. MC carbides decompose into the matrix during HIP and solid solution treatment, and  $M_{23}C_6$  carbides reprecipitate at GBs during aging [10–14].

Hence, the results show that the principal carbides in 15C are still MC and  $M_{23}C_6$  types, but significantly more of them appear than in 11C. The results also reveal that carbon addition in the fine-grain process produces no significant differences in carbide size and shape. The average length and aspect ratio of carbides in 15C are similar to those in 11C. This indicates that the lower pouring temperature in the fine-grain process reduces the temperature gra-

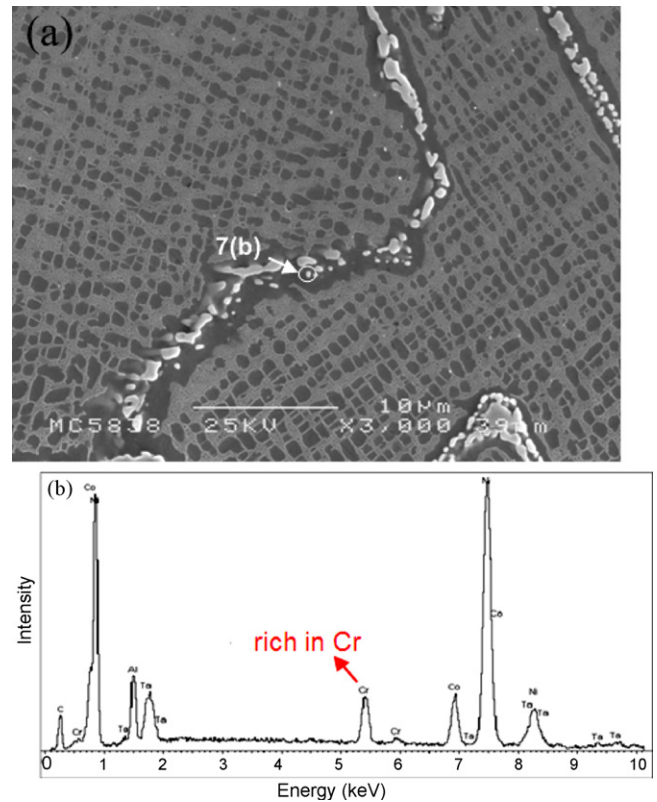


**Fig. 7.** (a) SEM images showing the carbides at GBs in 15C with EDS spectra in (b) from the carbides arrowed in (a).

dent and shortens the solidification time, limiting carbide growth [15].

#### 4.3. $\gamma$ - $\gamma'$ eutectic phase

The results show that carbon addition significantly reduces the area fraction of  $\gamma$ - $\gamma'$  eutectic phase from 8.6 to 5.3%. One of the reasons is that, while the  $\gamma$ - $\gamma'$  eutectic phases and carbides both form during solidification, the carbides form at an earlier stage of solidification, and eutectic phases form at the end of solidification [15–17]. Because the carbides form earlier and occupy the formation position of eutectic phases in the liquid pool, carbon addition reduces the area fraction of the eutectic phase [16]. Another possible reason is that the main elements enhancing the formation of the eutectic phases are Al, Ta, Hf, and Ti. As the eutectic phase forming elements of Ta and Hf are consumed by formation of (Ta, Hf)C carbides, the final amount of  $\gamma$ - $\gamma'$  eutectic phase is reduced [16].

#### 4.4. Tensile properties and fracture modes

The carbides play a very important role in superalloys. The amount, size and shape of carbides have the decisive effect on mechanical properties [4–8]. The experimental results show that the tensile strength, yield strength, and elongation of 15C at 760 °C are better than those of 11C. The most likely cause is that the addition of carbon greatly increases the amount of carbides. The higher amount of particle-like  $M_{23}C_6$  carbides precipitated at GBs could increase the strength of GBs and improve the mechanical properties, since  $M_{23}C_6$  carbides can postpone crack extension and avoid the GB sliding [6–8,10,11,18].

The literature [16] mentions that the  $\gamma$ - $\gamma'$  eutectic phase is a phase with lower strength. Thus, cracks typically originate in

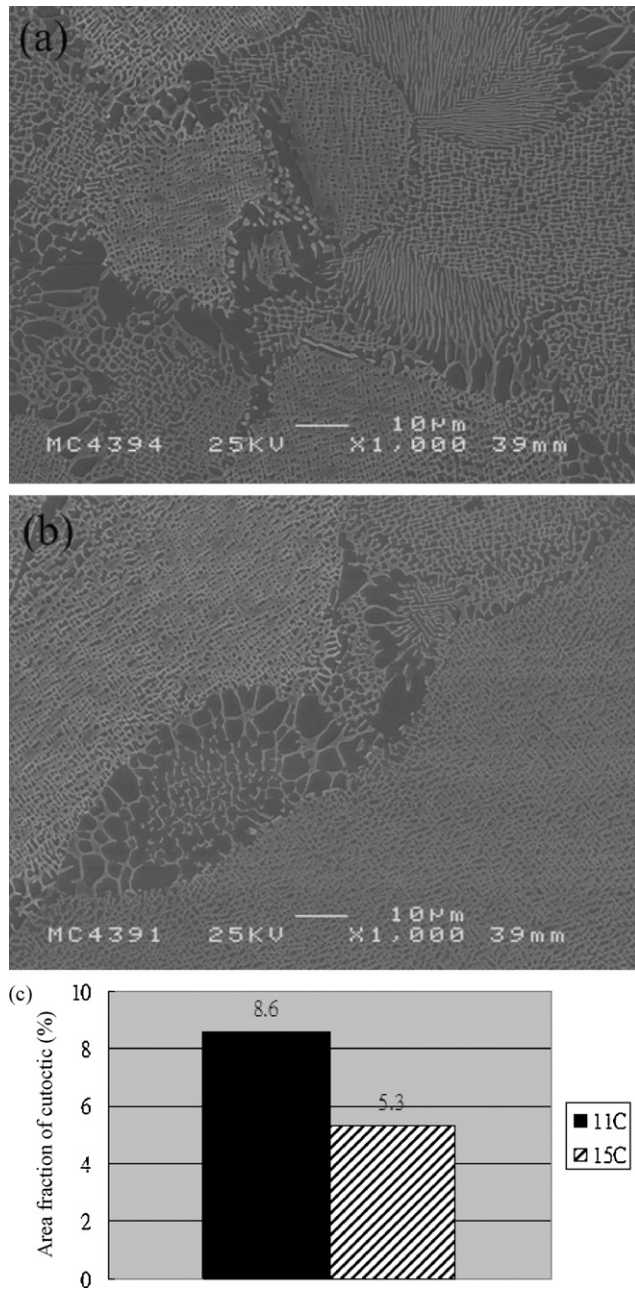


**Fig. 8.** SEM images showing the  $\gamma$ - $\gamma'$  phase morphology in (a) 11C and (b) 15C, and (c) the area fraction analysis results.

the  $\gamma$ - $\gamma'$  eutectic phase, and this phase also negatively affects the mechanical properties [16]. The area fraction of the  $\gamma$ - $\gamma'$  eutectic phase of 11C and 15C are known to be 8.6 and 5.3%, respectively. This indicates that the amount of weak  $\gamma$ - $\gamma'$  eutectic phase is reduced by increasing the carbon content, and that this effectively improves the yield strength, tensile strength, and elongation at 760 °C.

The fractographic observations of tensile tests at 760 °C show that the cracks in 11C were distributed mainly at GBs, and the fracture modes were typical intergranular fracture modes. After carbon was added, the GB strength of 15C was improved by more carbides precipitated at GBs. Hence, cracks in 15C were distributed mainly at both GBs and carbide/matrix interfaces. The tensile fracture modes of 15C were transgranular and intergranular mixed modes.

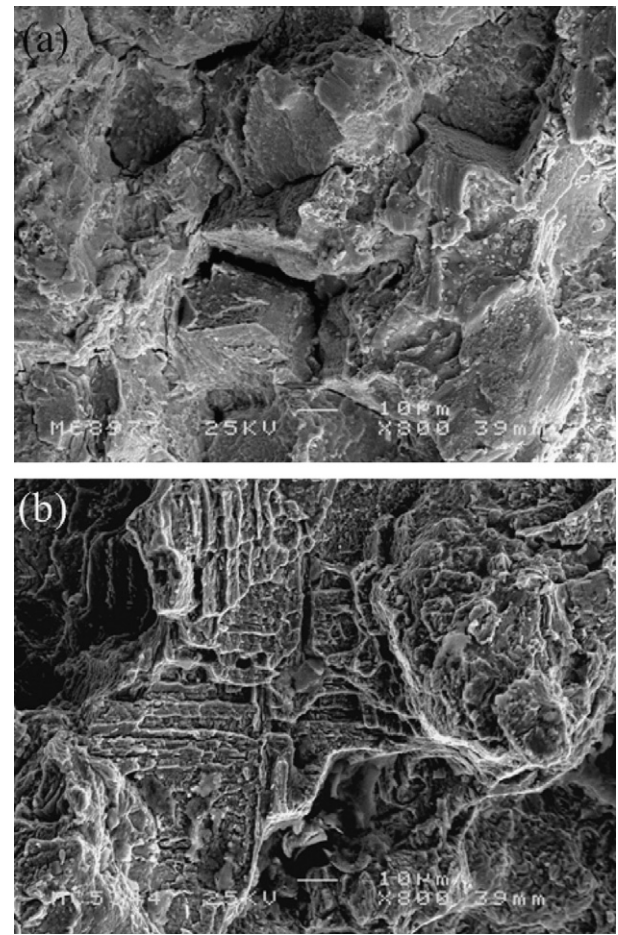


**Fig. 9.** Fracture surface SEM images of (a) 11C and (b) 15C following tensile test at 760 °C.

## 5. Conclusions

The effect of carbon content on the microstructure and tensile strength of fine-grain CM-681LC superalloy can be described as follows:

- (1) An increase in carbon content from 0.11 to 0.15 wt% produces no apparent effect on the melting point of CM-681LC superalloy. Further, no difference in grain size can be observed in the alloys obtained by the fine-grain casting process in this study.
- (2) MC carbides and  $M_{23}C_6$  carbides exist in CM-681LC superalloys with 0.11 and 0.15% carbon. Increasing the carbon content from 0.11 to 0.15 wt% increases the total area fraction of carbides considerably. However, the two alloys exhibit similar carbide shapes and sizes, probably because the short solidification time in the fine-grain process limits the growth of carbides.
- (3) The addition of carbon increases the amount of MC carbides, which not only consume the  $\gamma$ - $\gamma'$  eutectic phase forming elements of Ta and Hf in the matrix, but also occupy the position of  $\gamma$ - $\gamma'$  eutectic phases during solidification. Thus, carbon addition significantly reduces the area fraction of  $\gamma$ - $\gamma'$  eutectic phase from 8.6 to 5.3%.
- (4) An increase in the carbon content of CM-681LC nickel-base superalloy from 0.11 to 0.15 wt%, which increased the amount of carbides and decreased the  $\gamma$ - $\gamma'$  eutectic phases, improved the mechanical strength by about 6% and the elongation by about 50% in tensile tests at 760 °C.

## Acknowledgments

The authors would like to thank Mr. Y.P. Huang for his help in mechanical property evaluation. The equipment support of processing from Mr. J.S. Chen is also thankfully acknowledged.

## References

- [1] Harris, United States Patent 6,632,299 (2003).
- [2] J.M. Lane, *Adv. Mater. Process.* 137 (1990) 107–108.
- [3] L. Faxin, Y. Wenming, T. Xin, Y. Aide, C. Wanhua, *Mater. Eng. (China)* (1990) 7–11 (in Chinese).
- [4] A.K. Koul, W. Wallace, *Metal. Trans.* 13A (1982) 673.
- [5] Y.H. Kong, Q.Z. Chen, *Mater. Sci. Eng.* A366 (2004) 135–143.
- [6] J.S. Bae, J.H. Lee, S.S. Kim, C.Y. Jo, *Scr. Mater.* 45 (2001) 503–508.
- [7] R. Fernandez, J.C. Lecomte, T.E. Kattamis, *Metall. Trans.* A9 (1978) 1381–1386.
- [8] L. Liu, F. Sommer, H.Z. Fu, *Scr. Metall. Mater.* 30 (1994) 587–591.
- [9] J. Chen, J.H. Lee, C.Y. Jo, S.J. Choe, Y.T. Lee, *Mater. Sci. Eng.* A247 (1998) 113–125.
- [10] J. Yang, Q. Zheng, Z. Sun, H. Guan, Z. Hu, *Mater. Sci. Eng.* A429 (2006) 341–347.
- [11] C.N. Wei, H.Y. Bor, L. Chang, *Mater. Trans.* 49 (1) (2008) 193–201.
- [12] C.T. Sims, N.S. Stoloff, W.C. Hagel, *Superalloys II*, John Wiley & Sons, New York, 1987, p. 112.
- [13] B.G. Choi, I.S. Kim, D.H. Kim, C.Y. Jo, *Mater. Sci. Eng.* A478 (2008) 329–335.
- [14] J. Yang, Q. Zheng, H. Zhang, X. Sun, H. Guan, Z. Hu, *Mater. Sci. Eng.* A527 (2010) 1016–1021.
- [15] E.R. Cutler, A.J. Wasson, G.E. Fuchs, *Scr. Mater.* 58 (2008) 146–149.
- [16] L.R. Liu, T. Jin, N.R. Zhao, Z.H. Wang, X.F. Sun, H.R. Guan, Z.Q. Hu, *Mater. Lett.* 58 (2004) 2290–2294.
- [17] A.V. Shulga, *J. Alloys Compd.* 436 (2007) 155–160.
- [18] C.T. Sims, N.S. Stoloff, W.C. Hagel, *Superalloys II*, John Wiley & Sons, New York, 1987, p. 114.